ARTICLES
https://doi.org/10.1038/s41564-019-0391-z
nature microbiology

Bacterial fermentation and respiration processes are uncoupled in anoxic permeable sediments

Adam J. Kessler[1,2,7], Ya-Jou Chen[3,7], David W. Waite[4,5,7], Tess Hutchinson[1], Sharlynn Koh[1], M. Elena Popa[6], John Beardall[3], Philip Hugenholtz[4], Perran L. M. Cook[1*] and Chris Greening[3*]

Permeable (sandy) sediments cover half of the continental margin and are major regulators of oceanic carbon cycling. The microbial communities within these highly dynamic sediments frequently shift between oxic and anoxic states, and hence are less stratified than those in cohesive (muddy) sediments. A major question is, therefore, how these communities maintain metabolism during oxic–anoxic transitions. Here, we show that molecular hydrogen (H_2) accumulates in silicate sand sediments due to decoupling of bacterial fermentation and respiration processes following anoxia. In situ measurements show that H_2 is 250-fold supersaturated in the water column overlying these sediments and has an isotopic composition consistent with fermentative production. Genome-resolved shotgun metagenomic profiling suggests that the sands harbour diverse and specialized microbial communities with a high abundance of [NiFe]-hydrogenase genes. Hydrogenase profiles predict that H_2 is primarily produced by facultatively fermentative bacteria, including the dominant gammaproteobacterial family Woeseiaceae, and can be consumed by aerobic respiratory bacteria. Flow-through reactor and slurry experiments consistently demonstrate that H_2 is rapidly produced by fermentation following anoxia, immediately consumed by aerobic respiration following reaeration and consumed by sulfate reduction only during prolonged anoxia. Hydrogenotrophic sulfur, nitrate and nitrite reducers were also detected, although contrary to previous hypotheses there was limited capacity for microalgal fermentation. In combination, these experiments confirm that fermentation dominates anoxic carbon mineralization in these permeable sediments and, in contrast to the case in cohesive sediments, is largely uncoupled from anaerobic respiration. Frequent changes in oxygen availability in these sediments may have selected for metabolically flexible bacteria while excluding strict anaerobes.

At least half of the continental margin is covered by permeable sediments[1]. Defined as sands and gravels with permeabilities exceeding $1 \times 10^{-12}\,m^2$, these sediments are highly dynamic across space and time, especially in contrast to cohesive sediments (that is, muds and silts)[2]. Pore-water advection and physical disruptors (for example, tidal flows and groundwater discharge) drive continual exchange of dissolved particles, solutes and microorganisms between these sediments and the water column[3–5]. These sediments therefore shift between being oxic and anoxic over short distances and timescales, and rarely become as stratified in their redox chemistry as cohesive sediments[2,6–8]. It was long assumed that sands are less biogeochemically active than muds, given they harbour low levels of organic carbon. However, more recent studies have revealed that sands are highly active: most organic carbon produced by photoautotrophic and chemolithoautotrophic microorganisms is immediately mineralized by heterotrophs[2,9]. Cultivation-independent surveys have consistently shown that sands harbour phylogenetically and functionally diverse communities of prokaryotes and microbial eukaryotes[10–15]. Permeable sediments are now recognized as key systems for regulating global biogeochemical cycling and supporting oceanic primary production[2,16].

The biogeochemical processes and microbial communities that mediate carbon cycling are likely to differ between coastal permeable and cohesive sediments. In coastal muds, carbon mineralization pathways are highly stratified, with oxygen availability and redox potential decreasing with sediment depth. Within anoxic zones, organic carbon is primarily mineralized by obligately fermentative bacteria (for example, Clostridiales). The dominant end products, namely organic acids and molecular hydrogen (H_2), are oxidized by respiratory bacteria through redox cascades controlled by the concentration and energy yield of available oxidants[17,18]. H_2 is generally maintained at low steady-state concentrations (<2 nM) through tight coupling of fermentative H_2 producers (hydrogenogens) and respiratory H_2 consumers (hydrogenotrophs), notably sulfate reducers (for example, Desulfobacterales)[17,19,20]. Anoxic sands also maintain high mineralization rates, but the processes and communities responsible are unresolved[7,21]. Denitrification and sulfate reduction occur in such sediments, but measured rates for these processes vary and are often too low to account for carbon mineralization rates[21–30]. Other processes, namely iron reduction and methanogenesis, occur at low rates despite the availability of electron acceptors[21]. Hence, unlike cohesive sediments, anoxic mineralization processes in permeable sediments may not be principally governed by the availability of electron acceptors.

We have recently produced evidence that hydrogenogenic fermentation may be the dominant carbon mineralization pathway in anoxic permeable sediments. We used flow-through reactor (FTR) experiments to simulate shifts from oxic to anoxic conditions. Following the transition to anoxia, carbon mineralization rates were sustained and H_2 concomitantly accumulated to high levels (>1 μM). In contrast, low rates of respiration of sulfate, nitrate, nitrite and ferrous iron were observed[21]. Other recent

[1]Water Studies Centre, School of Chemistry, Monash University, Melbourne, Victoria, Australia. [2]School of Earth, Atmosphere & Environment, Monash University, Melbourne, Victoria, Australia. [3]School of Biological Sciences, Monash University, Melbourne, Victoria, Australia. [4]Australian Centre for Ecogenomics, School of Chemistry and Molecular Biosciences, The University of Queensland, St Lucia, Queensland, Australia. [5]School of Biological Sciences, University of Auckland, Auckland, New Zealand. [6]Institute for Marine and Atmospheric Research Utrecht, Utrecht University, Utrecht, The Netherlands. [7]These authors contributed equally: Adam J. Kessler, Ya-Jou Chen, David W. Waite. *e-mail: perran.cook@monash.edu; chris.greening@monash.edu

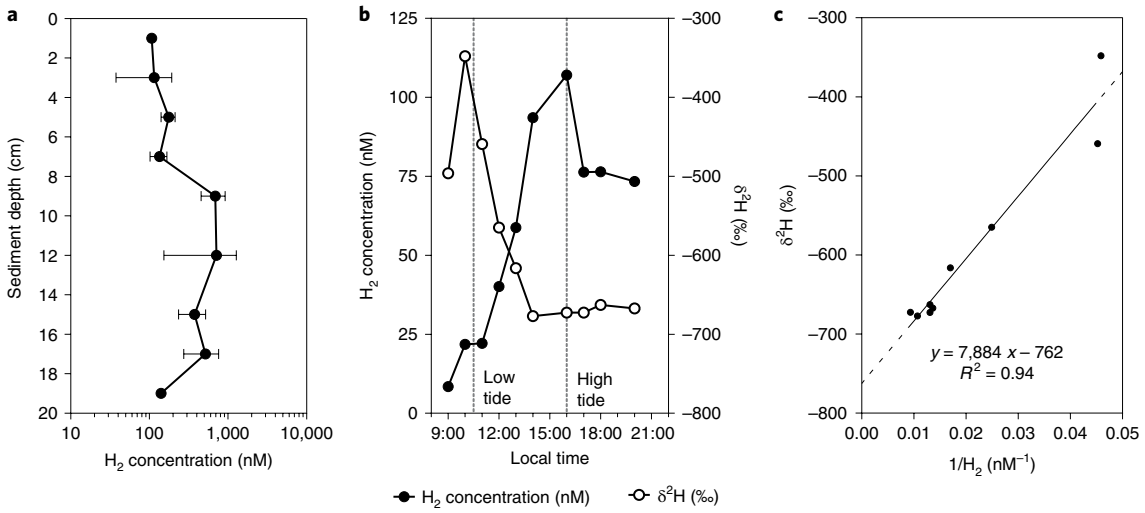

Fig. 1 | Biogenic H_2 accumulates in permeable sediments in situ. a, Pore-water concentrations of H_2 in subtidal sediment cores sliced every 2 cm. The centre values show mean concentrations and the error bars show standard deviations from three separate cores. **b**, Concentration and isotopic composition of H_2 from water samples overlying subtidal sediments. Samples were collected over an 11 h time course, including low tide (10:30) and high tide (16:00). **c**, A Keeling plot showing the isotopic composition (δ^2H) of the H_2 source in the water column. Data are from the time course from **b**, with an outlying value (9:00) excluded. The line was fitted by linear regression (ordinary least squares fit) and extrapolated (dashed lines) to the *y* intercept (-762.4 ± 18.8‰). R^2 values are based on the Pearson correlation coefficient.

studies have also emphasized the importance of fermentation in intertidal sand flats[22,31]. In the present study, we investigated how microbial communities in intertidal and subtidal silicate sand sediments from Port Philip Bay, Victoria, Australia adapt to hypoxia. We demonstrate that H_2 accumulates in situ and used biogeochemical and metagenomic approaches to resolve the processes and microorganisms responsible.

Results

Biologically produced H_2 accumulates in permeable sediments and overlying water columns. To determine whether H_2 production occurs in situ, we measured pore-water H_2 concentrations from subtidal silicate sand sediments at Middle Park Beach, Victoria, Australia. High levels of H_2 were detected at all depths in the three 20 cm cores analysed (Fig. 1a). Concentrations ranged from an average of 136 ± 76 nM in the upper 9 cm of each core to 511 ± 381 nM in the lower 11 cm. These concentrations are 340- to 1,280-fold greater than the atmosphere (0.55 ppmv; 0.41 nM dissolved in water)[32,33] and 2 orders of magnitude higher than typically reported in cohesive sediments[17,19,20].

In addition, we measured the dissolved and isotopic composition of H_2 in the water column overlying these sediments during a tidal cycle. H_2 concentrations increased from 21 nM at low tide (10:30; flow velocity = 9 cm s^{-1}) to 110 nM at peak high tide (16:00; flow velocity = 20 cm s^{-1}) and decreased thereafter (Fig. 1b). This suggests that disruption of the sediment by changing tides and currents stimulates net H_2 production. There was also a major shift in H_2 deuterium isotope ratios (δ^2H-H_2), from −350‰ to −670‰, concomitant with H_2 production (Fig. 1b). We generated a Keeling plot of the isotope ratios and concentrations of H_2 measured over the time course. From this, we extrapolated that δ^2H of the source is -762 ± 18‰ (Fig. 1c). Such a highly deuterium-depleted signature is compatible only with biological H_2 production: it is within the range of δ^2H values previously measured for microbial fermentation processes (-744 ± 17‰) and possibly biological nitrogen fixation (-637 ± 19‰)[34,35]. By contrast, it is incompatible with the δ^2H values reported for H_2 production from photochemical reactions ($+140 \pm 100$‰)[36,37] and combustion processes (-215 ± 125‰)[38,39].

Permeable sediments harbour diverse communities of facultatively fermentative H_2-producing bacteria and respiratory H_2-consuming bacteria. To infer the processes mediating H_2 production, we sequenced shotgun metagenomes from 5 samples, including shallow (2–5 cm) and deep (15–18 cm) sands from the intertidal and subtidal zones at the field site. Community analysis showed that the sands contain rich microbial communities (Fig. 2a and Supplementary Fig. 1): 46 microbial phyla were assigned from 16S ribosomal RNA gene metagenome reads (Supplementary Table 1) and 8,276 variants were detected by 16S amplicon sequencing (Supplementary Table 2). Reflecting the well-mixed nature of the sands, all five samples harboured a similar community composition (Figs. 2 and 3). The community appears to be dominated by lineages of aerobic chemoheterotrophic bacteria and, unlike cohesive sediments, contains few obligate fermenters, methanogens and homoacetogens (Fig. 2a and Supplementary Tables 1 and 2). In common with other nearshore permeable sediments[14,29,40], the most abundant families were Woeseiaceae (19.2%, Gammaproteobacteria) and Flavobacteriaceae (9.9%, Bacteroidia) (Fig. 2a and Supplementary Fig. 2). The other dominant classes were Alphaproteobacteria (8.5%), Deltaproteobacteria (3.4%) and Acidimicrobiia (2.2%), with phototrophic eukaryotes (chloroplasts, 1.9%) and sulfate-reducing bacteria (for example, Desulfobacterales, 0.7%) also detected. A combined metagenome assembly yielded 12 medium- or high-quality metagenome-assembled genomes (MAGs), covering 6.6% of total reads, including representatives of the five most abundant classes within the sediments (Supplementary Table 3 and Supplementary Figs. 3–11).

We subsequently measured the levels of key marker genes for fermentative and respiratory processes in the metagenome short and assembled reads (Fig. 2b and Supplementary Tables 3 and 4). The most abundant and prevalent genes were terminal oxidases and ATP synthases, indicating a predominantly aerobic respiratory community (Fig. 2b and Supplementary Table 3). [NiFe]-hydrogenases were also highly abundant, with an average count per million reads (120 CPM) of comparable magnitude to total 16S rRNA genes (200 CPM), suggesting that this type of hydrogenase is widely distributed in the sediment microbial communities and

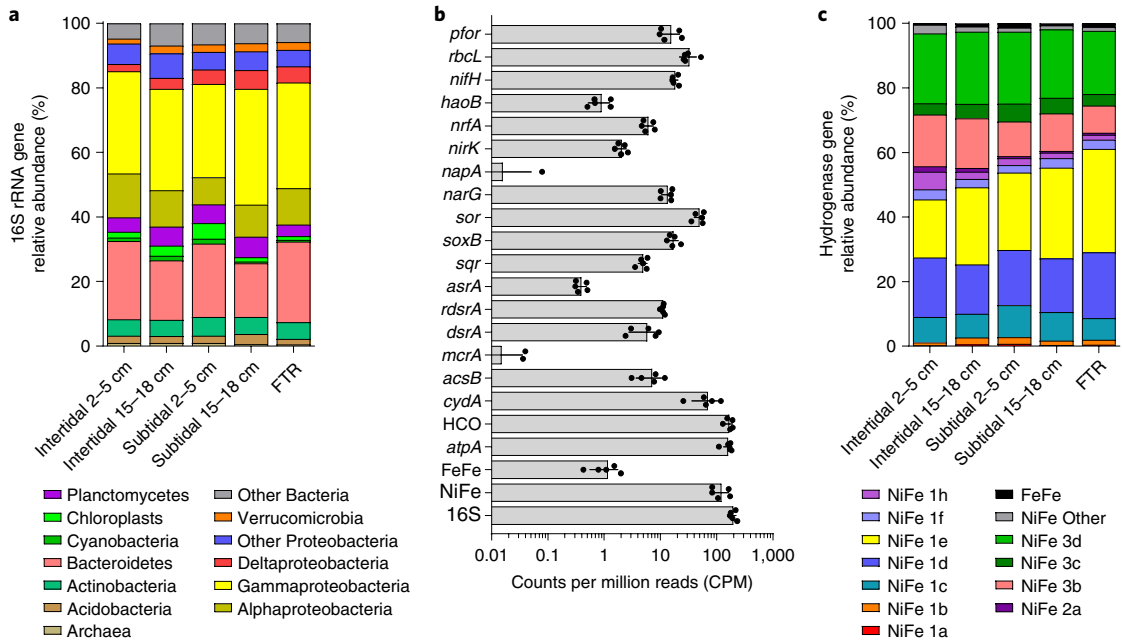

Fig. 2 | Permeable sediments harbour diverse H_2-metabolizing bacteria. a, Community composition of permeable sediments based on 16S reads retrieved from the five metagenomes. Eukaryotes and unassigned reads are not shown. Full taxonomic information is provided in Supplementary Tables 1 and 2. **b**, Functional capacity of permeable sediments based on normalized short-read count of genes encoding the catalytic subunits of key metabolic enzymes. The dots show read counts for each of the five metagenomes, the centre values show means and the error bars show standard deviations. 16S, 16S rRNA gene; NiFe, [NiFe]-hydrogenases; FeFe, [FeFe]-hydrogenases; *atpA*, ATP synthase; HCO, haem–copper oxidase genes (*coxA*, *cyoA* and *ccoN*); *cydA*, cytochrome *bd* oxidase; *acsB*, acetyl-CoA synthase; *mcrA*, methyl-CoM reductase; *dsrA* and *rdsrA*, reductive and oxidative clades of dissimilatory sulfite reductase; *asrA*, anaerobic sulfite reductase; *sqr*, sulfide–quinone oxidoreductase; *soxB*, thiosulfate hydrolase; *sor*, sulfur oxygenase/reductase; *narG*, dissimilatory nitrate reductase; *napA*, periplasmic nitrate reductase; *nirK*, dissimilatory nitrite reductase; *nrfA*, ammonifying nitrite reductase; *haoB*, hydroxylamine oxidoreductase; *nifH*, nitrogenase; *rbcL*, ribulose 1,5-bisphosphate carboxylase; *pfor*, pyruvate–ferredoxin oxidoreductase. Full counts are shown in Supplementary Table 4. **c**, Hydrogenase composition in the five metagenomes. The reads are divided into subtype as per the HydDB classification scheme, namely the oxidative group 1 and 2 [NiFe]-hydrogenases (groups 1a, 1b, 1c, 1d, 1e, 1f, 1h and 2a), bidirectional group 3 [NiFe]-hydrogenases (groups 3b, 3c and 3d), other [NiFe]-hydrogenases and the evolving [FeFe]-hydrogenases. Full counts are shown in Supplementary Tables 4 and 5.

is the main source of H_2 detected at the field sites. In contrast, the abundance of the H_2-producing enzymes nitrogenase and [FeFe]-hydrogenase is a hundred-fold lower (Fig. 2b and Supplementary Table 5). Also detected were genes for dissimilatory sulfate reduction (*dsrA*), stepwise denitrification (*narG* and *nirK*) and dissimilatory nitrate reduction to ammonium (*nrfA*) (Fig. 2b and Supplementary Table 6). The ecosystem also has capacity for oxidation of sulfur (*sor*), sulfide (*rdsrA*, *sqr*) and thiosulfate (*soxB*), and carbon fixation (*rbcL*) (Fig. 2b).

We classified the 27,260 hydrogenase sequences from the metagenomic short reads (Fig. 2c and Supplementary Table 4) and the 40 hydrogenase large-subunit sequences from the assembled reads (Fig. 3) using the functionally predictive scheme of HydDB[41,42]. While hydrogenases homologous to those of obligately anaerobic bacteria and phototrophic eukaryotes were detected, they comprised just 2% of total hydrogenase reads (Supplementary Table 4). Instead, group 3b and 3d [NiFe]-hydrogenases were the most abundant H_2-producing enzymes encoded in the metagenomes (Fig. 2c). These taxonomically widespread enzymes reversibly couple NAD(P)H oxidation to H_2 production and act as redox valves during adaptation of aerobic bacteria to anoxia[43–45]. MAGs from five different bacterial orders encoded such enzymes, namely Woeseiales, Polyangiales, Pseudomonadales, Microtrichales and the candidate actinobacterial order UBA5764 (Fig. 3b and Supplementary Fig. 12). In these genomes, the hydrogenase gene clusters co-occur with the determinants for aerobic heterotrophic growth (Supplementary Table 3). Hence, these organisms may stay energized by switching from hydrogenotrophic aerobic respiration when oxygenated to hydrogenogenic fermentation during anoxia. Two unbinned sequences with 66% identity to the group 3d hydrogenases of *Lutibacter* isolates (Flavobacteriaceae) were also detected (Fig. 3b).

The most abundant H_2-consuming enzymes are group 1e [NiFe]-hydrogenases (Fig. 2c). This enzyme is encoded by the Woeseiaceae MAG, in agreement with previous studies for this group[40], and multiple homologous sequences in the unbinned assembled reads (Fig. 3a and Supplementary Fig. 12). Such hydrogenases have previously been shown to support hydrogenotrophic sulfur respiration in Thiotrichales and Chromatiales[46,47], both of which are sister lineages to the Woeseiales. The community also encodes all four known classes of aerobic respiratory hydrogenases (1d, 1f, 1h and 2a), suggesting that oxic communities may recycle some of the H_2 produced in anoxic zones (Fig. 1d). While these sequences are underrepresented in the assembled reads, the Polyangiales MAG encoded a group 1f [NiFe]-hydrogenase and several unbinned reads shared 85% identity with group 1d [NiFe]-hydrogenases from *Lutibacter* isolate reads (Fig. 3a). Also present are [NiFe]-hydrogenase subgroups known to mediate sulfate (1a, 1b and 1c), nitrate (1c and 1d) and heterodisulfide (3c) respiration[41,48,49] (Fig. 2c). Consistently, the Desulfobulbaceae MAG encoded genes for a group 1b [NiFe]-hydrogenase (Supplementary Fig. 12).

Respiratory and fermentative processes become uncoupled in permeable sediments during oxic–anoxic transitions. We performed laboratory manipulation experiments to verify the pathways responsible for H_2 production and oxidation in permeable

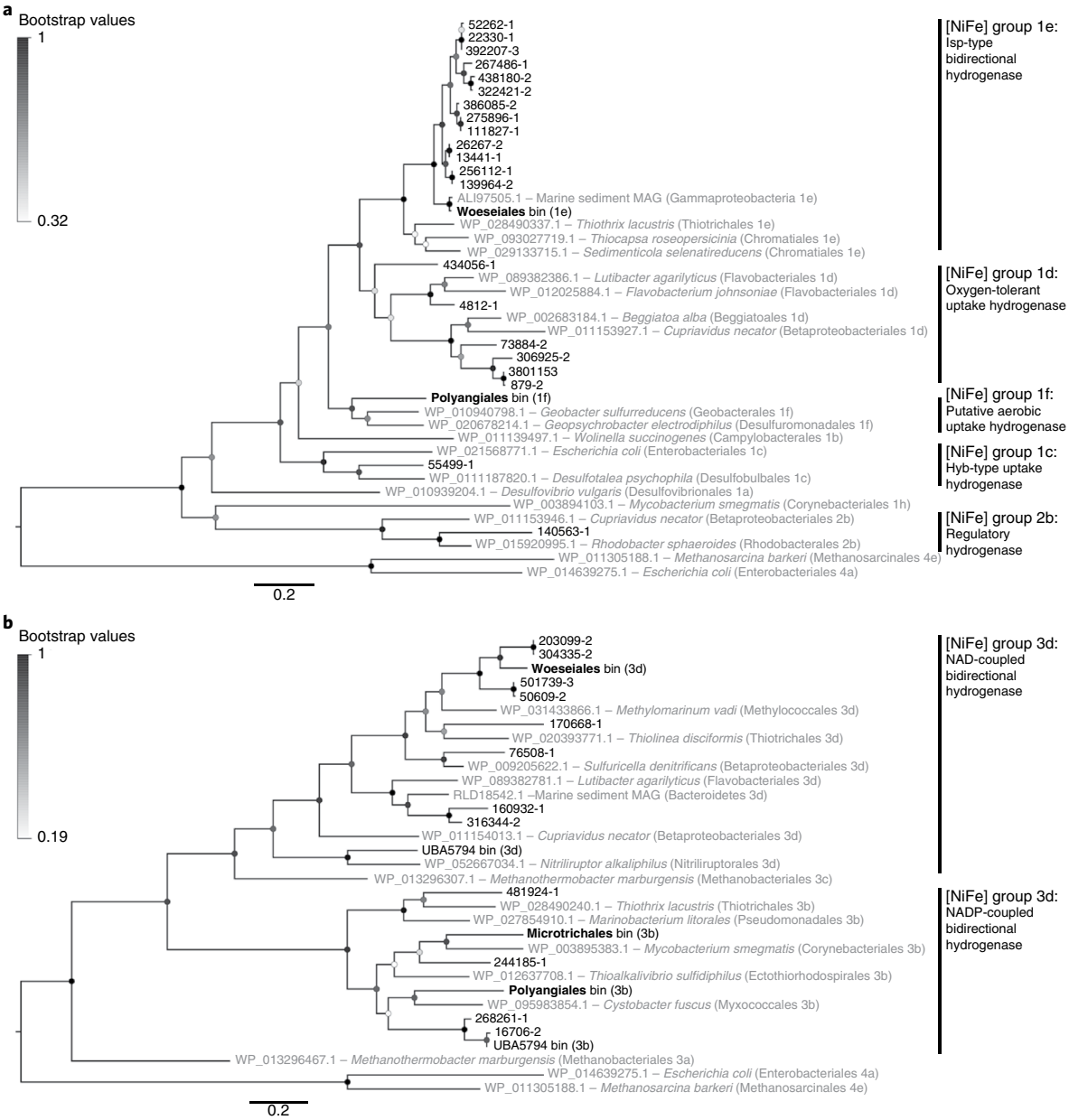

Fig. 3 | Phylogenetic analysis of hydrogenase genes. a, Phylogenetic tree of the group 1 and 2 [NiFe]-hydrogenase large-subunit protein sequences retrieved from the assembled unbinned reads (21 sequences) and metagenome-assembled genomes (2 sequences). **b**, Phylogenetic tree of the group 3 [NiFe]-hydrogenase large subunit retrieved from the assembled unbinned reads (12 sequences) and metagenome-assembled genomes (5 sequences). For **a** and **b**, sequences were aligned using Clustal, trees were constructed through the maximum-likelihood method (Poisson correction model, using all sites) and bootstrapping was performed with 200 replicates. Also shown are sequences for a well-characterized enzyme from each hydrogenase subgroup and the nearest reference genome hits to each metagenome sequence. The scale shows 0.2 amino acid substitutions per site.

sediments. First, we used FTRs to simulate the effect of oxic–anoxic transitions and pore-water advection on metabolic processes in surface sands. In the first 100 h following the transition to anoxia, net H_2 production was sustained at high rates (~2.2 μmol l^{-1} h^{-1}) in line with previous observations[21]. Hydrogen sulfide (H_2S), the end product of hydrogenotrophic sulfate reduction, was not initially detected despite electron donors (H_2) and electron acceptors (sulfate via seawater) being abundant in the system (Fig. 4a). This suggests that, following an oxic–anoxic transition, rates of hydrogenogenic fermentation greatly exceed hydrogenotrophic respiration in permeable sediments. Net H_2S production, concomitant with reduced net H_2 production, was observed only following 200 h of prolonged anoxia. Metagenomic analysis verified that the initial community composition and functional capacity of the FTR sample were similar to the in situ samples (Fig. 2a,b).

On the basis of the metagenome results, we performed a series of slurry experiments to monitor how changes in oxygen levels, electron donor availability and electron acceptor availability influence H_2 levels. Under oxic conditions, the microbial communities in the slurries consumed H_2 to sub-atmospheric levels (93 ± 51 pM). Net H_2 production was observed within 2 h following the transition to anoxia and peaked 48 h later (210 ± 37 nM) (Fig. 4b). In agreement with the FTR experiment results, rates of hydrogenogenic fermentation greatly exceeded those of hydrogenotrophic respiration under anoxic conditions. Net H_2 production was also observed in H_2-supplemented anoxic slurries using sands collected on three

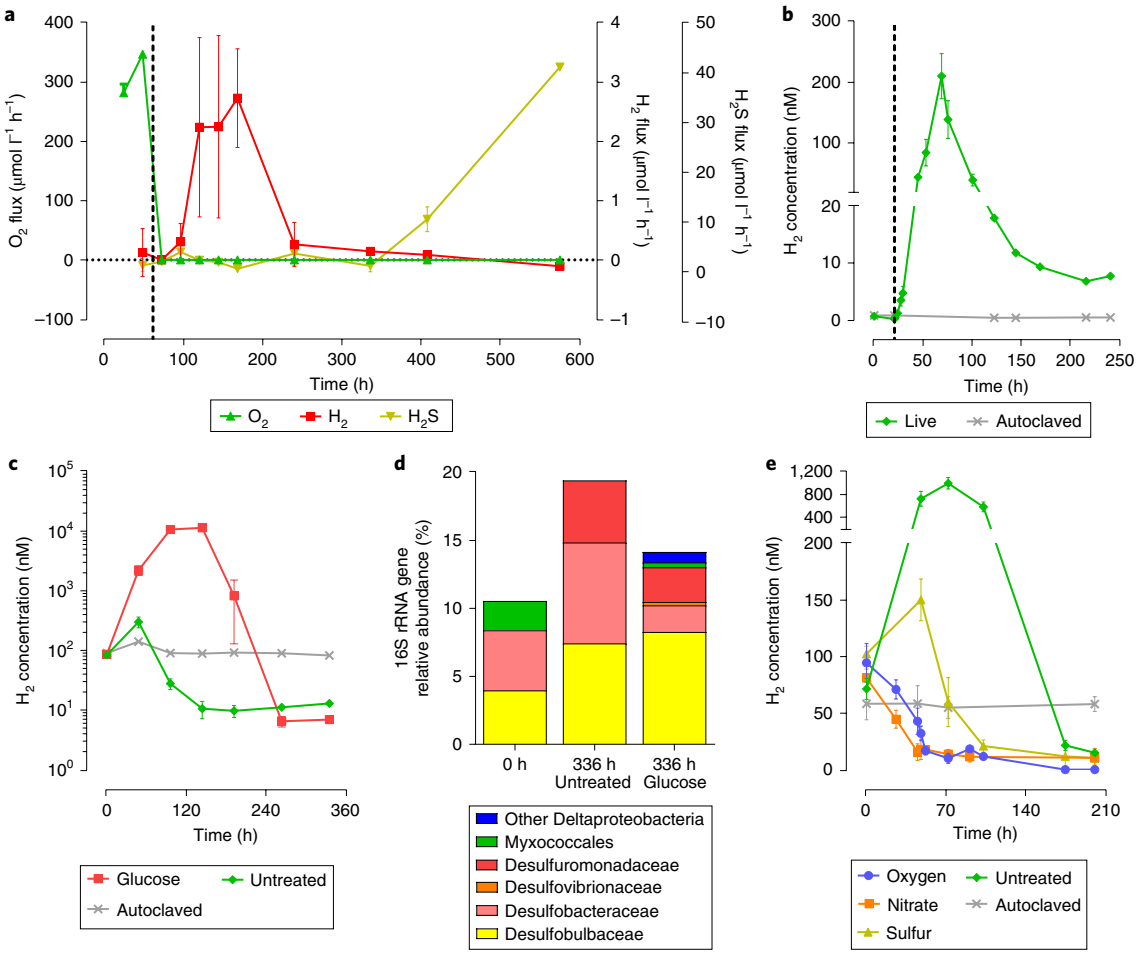

Fig. 4 | Fermentative and respiratory processes are uncoupled in permeable sediments. a, Measurement of fermentative and respiratory processes in FTRs during oxic–anoxic transitions. The FTRs were made anoxic immediately after sampling at 48 h by purging with argon. O_2, H_2 and H_2S were monitored. The centre values show means and the error bars show standard deviations from three independent FTRs. **b**, Slurry experiments detecting changes in H_2 concentrations in subtidal surface sediments (22 October 2018 samples) during an oxic–anoxic transition at 21 h. For **a** and **b**, the dotted line shows the time when the bioreactor and slurry were made anoxic. **c**, Slurry experiments detecting fermentative H_2 production in subtidal surface sediments (20 June 2018 samples). H_2 production rates were compared in anoxic slurries that were either untreated or supplemented with 1 mM glucose. The experiment used three independent slurries. **d**, Relative abundance of Deltaproteobacteria in sediments from **c** before and after incubation. Community structure was determined by 16S rRNA gene amplicon sequencing and full phylum-level composition is shown in Supplementary Fig. 14. **e**, Slurry experiments detecting respiratory H_2 consumption in subtidal surface sediments (30 April 2018 samples). Anoxic slurries were amended to give starting concentrations of either 16 mM elemental sulfur or 1 mM sodium nitrate. The study used six independent slurries. The levels of sulfide production and N_2 production in these slurries are shown in Supplementary Figs. 15 and 16. For **b**, **c** and **e**, the centre values show means and the error bars show standard deviations. For autoclaved controls, values show one control per treatment.

other occasions (Fig. 4c,e and Supplementary Fig. 13). Addition of the fermentable carbon source glucose stimulated H_2 production 16-fold and caused H_2 concentrations to exceed 10 μM (Fig. 4c). Analysis of community composition showed that glucose addition enriched a bacterium from the family Flavobacteriaceae (*Lutibacter* sp.) (Supplementary Fig. 14), which comprised 37% of the total community following two weeks of incubation; this is consistent with the tentative inference from the metagenomic assembled reads that some members of the Flavobacteriaceae encode the capacity for hydrogenogenic fermentation in permeable sediments.

During prolonged incubations under anoxic conditions, we detected activity of hydrogenotrophic sulfate reducers (using sulfate dissolved in seawater). Slurries become net H_2-consuming within 51 h (untreated) and 144 h (glucose treated) following the onset of anoxia, with H_2 levels decreasing to a steady-state concentration of 7 nM (Fig. 4b,c and Supplementary Fig. 13). This consumption occurred concurrently with sulfide production (~30 μM) (Fig. 4d). The relative abundance of three families of sulfate-reducing bacteria increased by the end of the incubation periods, Desulfobacteraceae, Desulfobulbaceae and Desulfovibrionaceae (Fig. 4d and Supplementary Fig 6). Addition of sodium molybdate, a potent inhibitor of sulfate reduction[50,51], caused H_2 to reaccumulate by disrupting coupling between hydrogenogenic fermenters and hydrogenotrophic sulfate reducers (Supplementary Fig. 13). Altogether, these findings suggest that inhibition of hydrogenotrophic sulfate reducers during oxygenation events is a major reason why H_2 accumulates in permeable sediments.

In agreement with the findings from the metagenomes, addition of a range of electron acceptors stimulated hydrogenotrophic respiration in the sand communities. In oxic slurries, most of the H_2 added at the start of the experiment (~100 nM) was consumed within 52 h (Fig. 4e). This is congruent with the abundance of aerobic bacteria harbouring aerobic respiratory uptake

[NiFe]-hydrogenases in the metagenome (Figs. 2 and 3). As also predicted from the metagenomes, addition of elemental sulfur and nitrate stimulated H_2 consumption in anoxic slurries (Fig. 4e). The end products of hydrogenotrophic sulfur reduction (H_2S) and stepwise denitrification (N_2) accumulated to micromolar levels during the time course (Supplementary Figs. 15 and 16); probably due to the high background levels of hydrogenogenic fermentation, the rates of net production of H_2S and N_2 exceeded the rates of net H_2 consumption under these conditions. Thiosulfate and sulfide addition also stimulated H_2 consumption relative to the untreated slurries (Supplementary Fig. 17). Thus, a second factor driving H_2 accumulation in these sediments is the limitation of hydrogenotrophic aerobes, nitrate reducers and sulfur reducers for electron acceptors.

In combination, our results indicate that H_2 production in permeable sediments is primarily mediated by bacteria, rather than microalgal eukaryotes as previously suggested[21]. Few eukaryotic-type [FeFe]-hydrogenases could be detected (Supplementary Tables 4 and 5), despite diatoms being moderately abundant in the community (Supplementary Tables 1 and 2). To address this discrepancy, we measured rates of H_2 production of cultures of two diatom species (*Navicula* and *Fragilariopsis*) previously isolated from Port Phillip Bay and shown to mediate H_2 production[21]. Both cultures mediated moderate levels of H_2 production under both light oxic and dark anoxic conditions. However, following administration of a cocktail of four antibiotics, this activity ceased under light oxic conditions and decreased 3.4-fold under dark anoxic conditions (Supplementary Fig. 18). We therefore propose diatom-associated bacteria, rather than diatoms themselves, mediate H_2 production through hydrogenase or nitrogenase activity. 16S rRNA gene community profiling revealed that a range of bacterial orders were consistently present in the cultures (Supplementary Fig. 19); most reads were from marine bacteria known to associate with diatoms[52], including Flavobacteriaceae. Moreover, we confirmed that the [FeFe]-hydrogenase maturation genes are absent from the eight sequenced Bacillariophyta genomes (Supplementary Table 7), suggesting that diatoms lack the genetic capacity to produce H_2.

Discussion

Fermentation and respiratory processes are uncoupled in well-mixed permeable sediments. Building on ex situ observations[21], in situ measurements show that H_2 is 750-fold oversaturated in sediment pore water and 50- to 250-fold oversaturated in overlying water columns relative to the atmosphere. It is extraordinary to detect such high levels of biologically produced H_2 in natural ecosystems. In oxic coastal surface waters, H_2 concentrations are typically less than tenfold oversaturated[53,54]. Moreover, in other ecosystems where H_2 metabolism predominates, such as cohesive coastal sediments, H_2 is maintained at a low steady-state concentration through tight coupling between hydrogenogenic and hydrogenotropic microorganisms[17,19,41]. Subsequent studies were used to infer the processes and microorganisms responsible for H_2 production. In common with cohesive sediments, hydrogenogenic fermenters and hydrogenotrophic sulfate reducers were present in sands. However, fermentation rates greatly exceeded those of sulfate reduction following oxic to anoxic transitions in laboratory experiments; these processes became tightly coupled only during prolonged anoxic incubations (two days in slurry experiments, eight days in FTR experiments). Given these findings, we predict that the spatial and temporal dynamics of permeable sediments cause fermenters and sulfate reducers to become uncoupled. Well-mixed sands, such as those in our field site, undergo frequent but irregular shifts between oxic and anoxic states through tidal flows and other physical processes[31,55,56]. These transitions, by favouring activity of facultatively anaerobic fermenters over obligately anaerobic sulfate reducers, drive net H_2 accumulation. Through work on similar sites, we have previously shown that the pore-water flow and transport field severely limits interactions between oxic and anoxic pore water[56]. Hence, contrary to cohesive sediments, H_2 is likely to accumulate in anoxic zones without being reoxidized. Moreover, advection may facilitate the transport of H_2 from pore water into the overlying water column, as has also been observed for other microbial products[29,57,58]. We cannot exclude the possibility that inputs into the system from rainfall or groundwater also influence H_2 cycling dynamics.

In turn, we predict that the dynamic nature of permeable sediments has selected for a community dominated by facultative fermenters. Metagenomic analysis indicated that shallow and deep sands from both tidal zones harbour similar community structures and functional capabilities, indicating that the microbial communities are sufficiently metabolically flexible to survive in both oxic and anoxic sands. The most abundant family in these sediments, the Woeseiaceae, encode enzymes for aerobic organotrophic and lithotrophic growth together with those for fermentative H_2 production. Five other abundant orders in these sediments, namely Polyangiales, Microtrichales, UBA5794, Pseudomonadales and tentatively Flavobacteriales, also encode genes for aerobic chemoheterotrophic respiration and hydrogenogenic fermentation. We predict that these bacteria persist in anoxic sands through fermentation of internal storage compounds or external carbon sources, and use group 3b and 3d [NiFe]-hydrogenases to directly couple reoxidation of reduced cofactors to the production of the redox sink H_2. These capabilities, in conjunction with previously described physiological traits relating to polysaccharide, nitrogen and sulfur utilization[29,40,59,60], have probably contributed to the success and abundance of these groups in coastal sediments. In stark contrast to cohesive sediments, very few obligate fermenters were detected, probably due to their inability to compete in transiently oxygenated ecosystems. Our previous hypothesis that phototrophic eukaryotes primarily mediate H_2 production in permeable sediments was not supported[21]. Molecular analyses detected few eukaryote-type [FeFe]-hydrogenases and culture-based analyses indicated that diatom-associated bacteria, rather than diatoms themselves, account for previous observations of H_2 production in diatom cultures[21]. Given their high biomass in permeable sediments[11,21], it is nevertheless likely that these phototrophs significantly contribute to anoxic carbon degradation and may form symbiotic associations with hydrogenogenic bacteria.

Bacterial communities within permeable sediments will respire H_2 when electron acceptors are available. We demonstrated through biogeochemical perturbation studies that the electron acceptors oxygen, sulfur and nitrate all support high rates of hydrogenotrophic respiration. Supporting this observation, half of the [NiFe]-hydrogenases detected in permeable sediment metagenomes are known to support aerobic respiration (groups 1d, 1f, 1h and 2a) and sulfur respiration (group 1e). In the oxic zone, bacteria capable of autotrophic or mixotrophic growth on H_2 may serve as significant sinks of fermentatively derived H_2; this process may contribute to the steep decreases in H_2 concentration observed between deep and shallow sands in the sediment cores. In addition, in line with the presence of the high-affinity group 1f and 1h hydrogenase lineages[32,61,62], the communities within these sediments can also oxidize H_2 at sub-atmospheric concentrations. Our data also strongly suggest that Woeseiaceae within these sediments reduce elemental sulfur to sulfides using H_2 as an electron donor. While the importance of sulfur oxidation by this family has recently been recognized in oxic sands[12], the role of anoxic sulfur reduction has been overlooked. Further studies are needed to understand the dynamics of sulfur metabolism in this system, including the possibility of cryptic cycling[63]. Nitrogen cycling in sands, which has long focused on heterotrophic denitrification[24–27], should also be re-examined with a focus on hydrogenotrophic denitrification and ammonification.

Given that this study focused on a single site, further work is needed to test the generalities of the phenomena described here. Other studies have shown that H_2-metabolizing orders described here are abundant at other sites, including Woeseiales, Flavobacteriales, Polyangiales and Desulfobacteriales[10,12,14,40], and have provided evidence of the presence and activity of hydrogenases[22,30,31,40]. Hence, H_2 metabolism may have a central role in the biogeochemistry and microbial ecology of permeable sediments worldwide. Nevertheless, the extent of coupling between fermentation and respiratory processes is likely to vary between sites. Two factors appear to limit respiratory H_2 consumption at our field site: inhibition of sulfate-reducers due to oxygenation during physical disturbance events and limitation of hydrogenotrophic aerobes, sulfur reducers and nitrate reducers for electron acceptors. However, the significance of these factors elsewhere will vary depending on physicochemical factors such as tidal intensity, sand permeability and electron acceptor availability. For example, tidal flats of the Wadden Sea appear to host a higher proportion of sulfate-reducing bacteria and mediate higher rates of hydrogenotrophic sulfate reduction[30,31]. Overall, we conclude that sands harbour specialized but versatile microbial communities that frequently shift between fermentation and respiration processes to accommodate environmental conditions. Moreover, in contrast to cohesive sediments, the processes and communities responsible for carbon mineralization appear to be controlled primarily by temporal rather than spatial factors.

Methods

Field site. Field work was conducted at Middle Park Beach, Melbourne, Australia (37.852425 S, 144.957519 E). Sediments from this site were previously shown to mediate high levels of H_2 production ex situ[21]. For sediment collection, samples were collected from well-mixed silicate sands from both the subtidal zone (~1 m deep at low tide) and intertidal zone (~1 m deep at high tide) using polyacrylamide cores (20 cm depth, 6.7 cm inner diameter). Samples for the water-column time series, metagenome sequencing and FTR experiments were collected on 28 October 2016. Samples for successive slurry experiments were collected on four separate dates in 2018, namely 10 April, 30 April, 20 June and 22 October. Samples were also collected for pore-water H_2 concentration analysis on 28 February 2018.

Sediment depth profiles. Three sediment cores of 20 cm depth were collected from subtidal sands during the February 2018 field trip. Within 2 h of collection, cores were carefully extruded and segmented into 2 cm slices. They were immediately transferred to beakers containing 30 ml Ar-purged carbonate-free artificial seawater supplemented with 2% $ZnCl_2$. The slices were gently stirred to homogenize the pore water with the artificial seawater. Three millilitres of the solution was transferred to a gas-tight vial and 1.5 ml of the liquid was replaced with a He headspace. After equilibration, H_2 content was analysed using a Model 8610 Gas Chromatograph (SRI Instruments) fitted with a reduction gas detector. Ultrapure helium (99.999% He) was used as a carrier gas at a flow rate of 10 ml min^{-1}. The valve heating oven, injector, column oven and detector temperature were 80 °C, 70 °C, 70 °C and 295 °C, respectively. The instrument was calibrated using dilutions of an ultrapure 1% H_2 standard in N_2. PeakSimple 2000 chromatography integration software was used to acquire chromatograms and derive concentrations. Whereas strong signals were measured in the sediment samples, H_2 concentrations in procedural blanks, containing only argon-purged $ZnCl_2$-supplemented artificial seawater, were below the detection limits of the machine (~2 nM). Sub-atmospheric concentrations of H_2 were measured in the 22 October slurry experiment using a customized trace gas analyser (model TGA-6791-W-4U-2, Valco Instruments Company Inc.) containing a pulsed discharge helium ionization detector[64].

Water-column time series. Water-column samples were collected from beyond the wash zone (~1 m deep) during the October 2016 field trip. Water samples (500 ml) were drawn up from approximately 50 cm below the surface using a 1.6 l polycarbonate syringe. The remainder of the syringe was filled with ambient air. The syringe was then sealed and shaken vigorously for 2 min to transfer the H_2 to the gas phase. The headspace was transferred to an evacuated 1 l glass flask for later analysis. Samples were collected every hour over an 11 h period that encompassed low tide and high tide. Samples of air were also taken to correct for atmospheric hydrogen concentrations and isotope ratios measured in the headspace. H_2 concentrations and H_2 isotope ratios (δ^2H-H_2) from the headspace gas were analysed by continuous flow isotope ratio mass spectrometry using a ThermoFinnigan Delta Plus XL instrument as previously described[65,66]. The results were calibrated using a gas standard of known H_2 mole fraction and isotopic composition (500 ppbv, δ^2H = +95‰ Vienna Standard Mean Ocean Water). The mole fraction results are reported with an uncertainty of 1%, and the isotope ratios have a typical uncertainty of 1‰. Note that, due to the rapid equilibration between H_2 and H_2O, H_2 fractionation (δ^2H-H_2) is typically presented relative to water (δ^2H-H_2O). We did not measure δ^2H-H_2O concurrently with our measurements of δ^2H-H_2, but we have measured δ^2H-H_2O at the same site as +5.7 ± 0.8‰ Vienna Standard Mean Ocean Water (analysed in triplicate using a Thermo Finnigan H-Device coupled to a Thermo Finnigan Delta Plus Advantage gas source mass spectrometer). As this is very close to zero compared with our values of δ^2H-H_2, any relative errors caused by not presenting this offset are likely to be less than 1%.

Community DNA extraction. Total community DNA was extracted from two intertidal core samples (2–5 cm and 15–18 cm), two subtidal core samples (2–5 cm and 15–18 cm) and a day-1 FTR sample (0–10 cm) collected during the October 2016 field trip. DNA was extracted from 0.3 g of wet sediment samples using the MoBio PowerSoil Isolation kit according to the manufacturer's instructions. Samples were eluted in DNase- and RNase-free UltraPure Water (Thermo Fisher Scientific). A sample-free negative control was also run. Nucleic acid purity and yield were confirmed using a Nanodrop 1000 and Qubit Fluorometer.

Metagenome sequencing and assembly. Metagenomic shotgun libraries were prepared for each of the five samples using the Nextera XT DNA Sample Preparation Kit (Illumina Inc.). Sequencing was performed on an Illumina NextSeq500 platform with 2 × 150 base pair High Output run chemistry. A total of 144,525,216 reads were obtained across the five samples. In contrast, the read counts for the negative controls were 6,547 (extraction control) and 1,360 (library preparation control). Raw sequence reads in each sample were stripped of adapter and barcode sequences, and then contaminating PhiX sequences were identified and removed using the BBDuk function of BBTools v36.92 (https://sourceforge.net/projects/bbmap/) with a *k*-mer size of 31 and a Hamming distance of 1. Retained read pairs were then quality-trimmed using BBDuk with $Q > 20$. Quality filtering yielded a total of 140,479,970 paired and 3,613,688 singleton reads, with 89.6% of the original sequences passing quality control. The metagenomes were assembled both individually and collectively using SPAdes v.3.11.1[67] and short reads were mapped to the resulting assembly using BamM v1.7.3 with default parameters (http://ecogenomics.github.io/BamM). Co-assembled sequences were then binned into MAGs using three independent binning tools: MetaBAT v2.12.1[68], MaxBin v.2.2.4[69] and GroopM v0.3.0[70]. Raw bins were then dereplicated at the contig level using DAS_Tool v1.1.1[71], and then further dereplicated according to ANI with dRep v2.0.5[72]. The resulting MAGs were assessed for completeness and contamination using CheckM v1.0.11[73], and manually curated using RefineM (https://github.com/dparks1134/RefineM). Twelve MAGs satisfied the conditions[74] of a medium-quality genome (completeness >50%, contamination <10%) or high-quality genome (completeness >90%, contamination <5%) (Supplementary Table 3). The others were rejected and returned to the pool of unbinned assembled sequences. Initial taxonomic classification of the MAG was performed by identifying partial 16S and 23S rRNA gene sequences using RNAmmer v1.2[75]. Predicted sequences were aligned using the SINA web aligner[76] and inserted into the SILVA SSU and LSU v132 databases[77]. Placement according to the 16S rRNA gene fragment was further examined using the Genome Taxonomy Database[78] to infer a phylogenetic tree from a concatenation of 120 conserved bacterial marker proteins. Initial taxonomy assignment was performed using the GTDB-TK pipeline (https://github.com/Ecogenomics/GtdbTk), which was then refined using maximum-likelihood phylogenetic inference of each MAG using IQ-Tree[79] with the LG + G model of amino-acid substitution and 100 bootstrap resamplings to assess node stability. For the binned and unbinned assembled sequences, open reading frames were predicted using Prodigal v2.6.3[80] and annotated against the Pfam v31.0 and TIGRfam v15.0 databases using hmmer v3.1b2[81].

Community analysis. Community composition profiles were generated by retrieving and assigning 16S rRNA genes from the five metagenomes. Putative 16S sequence fragments were retrieved using GraftM[82], and then aligned to 16S secondary structure in mothur[83] to verify the accuracy of predictions. Sequences that were successfully aligned were then classified using the naive Bayesian method against the SILVA SSU v132 database[77]. To provide a high-resolution community profile, the five samples were also subjected to 16S rRNA gene amplicon sequencing. The hypervariable V4 region of the 16S rRNA gene was amplified using the primer pair 515F/806R[84] and paired-end sequencing was performed using an Illumina MiSeq (Australian Centre for Ecogenomics). Raw sequences were processed using the deblur pipeline on the QIIME 2 platform[85] to resolve amplicon sequence variants[86]. Three samples from the slurry analysis and two samples from the diatom studies were also subject to DNA extraction and 16S rRNA gene sequencing.

Functional annotation. The relative abundance of metabolic marker genes was determined in the quality-filtered unassembled reads through a combination of hidden Markov models (HMMs) and homology-based searches. HMM searches were performed against the Panther, Pfam and TIGRfam databases as described above using hmmer v3.1b2[81]. From the bulk annotation, we identified genes

involved in oxidative phosphorylation (*atpA*), aerobic respiration (*ccoN*, *coxA*, *cyoA* and *cydA*), nitrogen cycling (*haoB*, *napA*, *narG*, *nifH*, *nirK*, *nirS* and *nrfA*), sulfur cycling (*asrA*, *soxB*, *sqr* and *sor*), methanogenesis (*mcrA*), acetogenesis (*acsB*), fermentation (*pfor*) and carbon fixation (*rbcL*). The HMM profiles used were described previously[87] with cutoff scores of 10^{-10}. Genes encoding the catalytic subunits of hydrogenases and dissimilatory sulfite reductases (*dsrA*) were retrieved through Diamond BLASTx queries against comprehensive custom databases[42,88]. Matches were accepted where total sequence identity exceeded 70% and BLAST *E*-values were less than 10^{-10}. Negative control samples were subjected to the same gene calling and annotation approaches, but did not return matches to any of the gene families examined in this study. Retrieved sequences were classified into hydrogenase subgroups (groups 1 to 4 [NiFe]-hydrogenases; groups A to C [FeFe]-hydrogenases) or *dsrA* types (oxidative or reductive) according to their closest hit in the reference databases. The 38 [NiFe]-hydrogenase large-subunit sequences present in the assembled reads were aligned with hydrogenase reference sequences using ClustalX[89]. Evolutionary relationships were visualized on neighbour-joining phylogenetic trees constructed in MEGA7[90] and bootstrapped with 498 replicates.

FTR experiments. FTRs were used to measure rates of aerobic respiration, H_2 production and H_2S production in permeable sediments during an oxic–anoxic transition. As described previously[21,24], each reactor comprises a short cylinder (4.2 cm length, 4.4 cm inner diameter) packed with sediment and circulated with seawater collected from the field site. Surface sediments were extracted from cores (0–10 cm) collected during the October 2016 field trip. Sediments were sieved through a 2 mm mesh to remove large debris, homogenized and packed into three FTRs. After loading sands into the FTR, a 1 g sample was extracted for metagenome analysis. Aerated seawater was recirculated through the FTRs from a 2 l glass bottle using a peristaltic pump at a flow rate of ~45 ml h^{-1}. Sampling was performed 48 h after beginning the experiment and every 24 h thereafter. After the first sampling (48 h), the reservoir was made anoxic by purging with argon. O_2 levels were monitored from the outlet of the FTRs using a flow-through O_2-sensitive probe (Pyroscience Firesting). To measure the biogeochemical reactions in the FTRs, 20 ml of water was collected at the FTR outlets using a glass syringe. Subsamples of this water were preserved for later analysis of H_2 (3 ml in gas-tight glass vial, preserved with 10 µl 6% $HgCl_2$) and H_2S (3 ml filtered in polypropylene vial, preserved with 100 µl 48 mM Zn acetate). H_2 concentrations were measured by gas chromatography (described above) and H_2S concentrations were measured in a GBC ultraviolet/visible spectrophotometer using the methylene blue method as previously described[91].

Slurry experiments. Slurry experiments were used to compare rates of H_2 consumption and production in surface sediments (0–10 cm). Each slurry comprised a 160 ml sealed vial containing 30 g sieved sand (wet weight), 70 ml filtered seawater collected from the field site and a 60 ml headspace. The headspace contained ambient air for oxic incubations and was purged with argon for anoxic incubations. Vials were incubated at room temperature on an orbital shaker (175 r.p.m.) to ensure that sediments were constantly in motion and well mixed. A 1 ml subsample of the headspace was removed at regular intervals over the time course, stored in a He-purged 3 ml glass vial and analysed for H_2 by gas chromatography (described above). Four separate slurry experiments were performed using subtidal surface sediments collected on different dates. For the sediments collected on 20 October 2018, H_2 concentrations were determined at regular time intervals in four independent slurries that initially contained an ambient air headspace and were purged with argon at 21 h. For the sediments collected on 20 June 2018, H_2 concentrations were compared in anoxic slurries supplemented with 80 nM H_2 in the presence and absence of 1 mM glucose. In this experiment, H_2 concentrations were analysed across three independent slurries per condition. For the sediments collected on 10 April 2018, H_2 concentrations were compared in oxic and anoxic slurries supplemented with 80 nM H_2. At 206 h, 20 mM sodium molybdate was added to inhibit sulfate reduction[50]. In this experiment, H_2 concentrations were analysed across five independent slurries per condition. For the sediments collected on 30 April 2018, H_2, N_2 and sulfide concentrations were measured after spiking slurries with 80 nM H_2 and different oxidants. H_2 concentrations were compared in oxic slurries, anoxic slurries and anoxic slurries treated with either 1 mM ^{15}N-labelled sodium nitrate ($Na^{15}NO_3$), 16 mM ground elemental sulfur, 20 mM sodium thiosulfate ($Na_2S_2O_3.5H_2O$) or 200 µM sodium sulfide. For the $Na^{15}NO_3$-treated samples, $^{15}N_2$ production was analysed using a Sercon isotope ratio mass spectrometer coupled to a gas chromatograph. Sulfide levels were measured through the methylene blue method (described above) by opening one slurry per time point and extracting 3 ml of liquid for analysis. Initially six replicates were prepared for each treatment, so that at the final sampling time triplicate measurements could be obtained even after several slurries were terminated for sulfide analysis. For each experiment, one autoclaved control was also run per condition, which confirmed that the different treatments did not influence H_2 concentration through abiotic processes.

Diatom culture experiments. The diatom studies used *Fragilariopsis* and *Navicula* cultures previously isolated from permeable sediments within Port Phillip Bay[21]. Pre-cultures inoculated from single colonies were treated with either a single antibiotic (100 µg ml^{-1} kanamycin) or an antibiotic cocktail (100 µg ml^{-1} kanamycin, 40 µg ml^{-1} ampicillin, 20 µg ml^{-1} streptomycin and 8 µg ml^{-1} tetracycline). Cultures were subsequently inoculated into 250 ml conical flasks containing 50 ml of f/2 medium[92] supplemented with 1% sodium nitrate and grown at 18 °C with continuous illumination (60 µmol photons m^{-2} s^{-1}) and agitation (150 r.p.m. on a magnetic stir plate). On reaching a density of 10^5 cells ml^{-1}, the 50 ml cultures were transferred into 125 ml sealed serum vials and incubated under either light oxic or dark anoxic conditions. For light oxic incubations, cultures were incubated under constant illumination in an ambient air headspace. For dark anoxic incubations, cultures were covered by aluminium foil and purged with helium gas. Headspace H_2 concentrations were measured daily by gas chromatography for ten days. At the end of the experiment, cells were collected by centrifugation (5,000×*g*, 20 min). Total community DNA was extracted using a modified Griffith's protocol[93] and subject to 16S rRNA gene amplicon sequencing as described above.

Reporting Summary. Further information on research design is available in the Nature Research Reporting Summary linked to this article.

Data availability

The data that support the findings of this study are available from the corresponding authors upon request. All sequencing data and MAGs have been uploaded to the Sequence Read Archive under BioProject accession number PRJNA515295.

Received: 22 August 2018; Accepted: 28 January 2019;
Published online: 11 March 2019

References

1. Hall, S. J. The continental shelf benthic ecosystem: current status, agents for change and future prospects. *Environ. Conserv.* **29**, 350–374 (2002).
2. Huettel, M., Berg, P. & Kostka, J. E. Benthic exchange and biogeochemical cycling in permeable sediments. *Annu. Rev. Mar. Sci.* **6**, 23–51 (2014).
3. Reimers, C. E. et al. *In situ* measurements of advective solute transport in permeable shelf sands. *Cont. Shelf Res.* **24**, 183–201 (2004).
4. Santos, I. R., Eyre, B. D. & Huettel, M. The driving forces of porewater and groundwater flow in permeable coastal sediments: a review. *Estuar. Coast. Shelf Sci.* **98**, 1–15 (2012).
5. Huettel, M., Ziebis, W. & Forster, S. Flow-induced uptake of particulate matter in permeable sediments. *Limnol. Oceanogr.* **41**, 309–322 (1996).
6. Glud, R. N. Oxygen dynamics of marine sediments. *Mar. Biol. Res.* **4**, 243–289 (2008).
7. Cook, P. L., Frank, W., Glud, R., Felix, J. & Markus, H. Benthic solute exchange and carbon mineralization in two shallow subtidal sandy sediments: effect of advective pore-water exchange. *Limnol. Oceanogr.* **52**, 1943–1963 (2007).
8. Ahmerkamp, S. et al. Regulation of benthic oxygen fluxes in permeable sediments of the coastal ocean. *Limnol. Oceanogr.* **62**, 1935–1954 (2017).
9. Boudreau, B. P. et al. Permeable marine sediments: overturning an old paradigm. *EOS Trans. Am. Geophys. Union* **82**, 133–136 (2001).
10. Gobet, A. et al. Diversity and dynamics of rare and of resident bacterial populations in coastal sands. *ISME J.* **6**, 542 (2012).
11. Böer, S. I., Arnosti, C., Van Beusekom, J. E. E. & Boetius, A. Temporal variations in microbial activities and carbon turnover in subtidal sandy sediments. *Biogeosciences* **6**, 1149–1165 (2009).
12. Dyksma, S. et al. Ubiquitous Gammaproteobacteria dominate dark carbon fixation in coastal sediments. *ISME J.* **10**, 1939 (2016).
13. Hunter, E. M., Mills, H. J. & Kostka, J. E. Microbial community diversity associated with carbon and nitrogen cycling in permeable shelf sediments. *Appl. Environ. Microbiol.* **72**, 5689–5701 (2006).
14. Probandt, D. et al. Permeability shapes bacterial communities in sublittoral surface sediments. *Environ. Microbiol.* **19**, 1584–1599 (2017).
15. Probandt, D., Eickhorst, T., Ellrott, A., Amann, R. & Knittel, K. Microbial life on a sand grain: from bulk sediment to single grains. *ISME J.* **12**, 623–633 (2017).
16. Devol, A. H. Denitrification, anammox, and N_2 production in marine sediments. *Annu. Rev. Mar. Sci.* **7**, 403–423 (2015).
17. Hoehler, T. M., Alperin, M. J., Albert, D. B. & Martens, C. S. Thermodynamic control on hydrogen concentrations in anoxic sediments. *Geochim. Cosmochim. Acta* **62**, 1745–1756 (1998).
18. Canfield, D. E., Thamdrup, B. & Hansen, J. W. The anaerobic degradation of organic matter in Danish coastal sediments: iron reduction, manganese reduction, and sulfate reduction. *Geochim. Cosmochim. Acta* **57**, 3867–3883 (1993).
19. Lovley, D. R. & Goodwin, S. Hydrogen concentrations as an indicator of the predominant terminal electron-accepting reactions in aquatic sediments. *Geochim. Cosmochim. Acta* **52**, 2993–3003 (1988).
20. Lin, Y.-S. et al. Towards constraining H_2 concentration in subseafloor sediment: a proposal for combined analysis by two distinct approaches. *Geochim. Cosmochim. Acta* **77**, 186–201 (2012).

21. Bourke, M. F. M. F. et al. Metabolism in anoxic permeable sediments is dominated by eukaryotic dark fermentation. *Nat. Geosci.* **10**, 30–35 (2017).
22. Chen, J. et al. Impacts of chemical gradients on microbial community structure. *ISME J.* **11**, 920 (2017).
23. Rao, A. M. F., McCarthy, M. J., Gardner, W. S. & Jahnke, R. A. Respiration and denitrification in permeable continental shelf deposits on the South Atlantic Bight: rates of carbon and nitrogen cycling from sediment column experiments. *Cont. Shelf Res.* **27**, 1801–1819 (2007).
24. Evrard, V., Glud, R. N. & Cook, P. L. M. The kinetics of denitrification in permeable sediments. *Biogeochemistry* **113**, 563–572 (2013).
25. Eyre, B. D., Santos, I. R. & Maher, D. T. Seasonal, daily and diel N_2 effluxes in permeable carbonate sediments. *Biogeosciences* **10**, 2601–2615 (2013).
26. Kessler, A. J. et al. Quantifying denitrification in rippled permeable sands through combined flume experiments and modeling. *Limnol. Oceanogr.* **57**, 1217–1232 (2012).
27. Marchant, H. K. et al. Coupled nitrification–denitrification leads to extensive N loss in subtidal permeable sediments. *Limnol. Oceanogr.* **61**, 1033–1048 (2016).
28. Marchant, H. K. et al. Denitrifying community in coastal sediments performs aerobic and anaerobic respiration simultaneously. *ISME J.* **11**, 1799 (2017).
29. Marchant, H. K. et al. Metabolic specialization of denitrifiers in permeable sediments controls N_2O emissions. *Environ. Microbiol.* **20**, 4486–4502 (2018).
30. Dyksma, S., Pjevac, P., Ovanesov, K. & Mussmann, M. Evidence for H_2 consumption by uncultured Desulfobacterales in coastal sediments. *Environ. Microbiol.* **20**, 450–461 (2018).
31. Saad, S. et al. Transient exposure to oxygen or nitrate reveals ecophysiology of fermentative and sulfate-reducing benthic microbial populations. *Environ. Microbiol.* **19**, 4866–4881 (2017).
32. Greening, C., Berney, M., Hards, K., Cook, G. M. & Conrad, R. A soil actinobacterium scavenges atmospheric H_2 using two membrane-associated, oxygen-dependent [NiFe] hydrogenases. *Proc. Natl Acad. Sci. USA* **111**, 4257–4261 (2014).
33. Novelli, P. C. et al. Molecular hydrogen in the troposphere: global distribution and budget. *J. Geophys. Res. Atmos.* **104**, 30427–30444 (1999).
34. Walter, S. et al. The stable isotopic signature of biologically produced molecular hydrogen (H_2). *Biogeosciences* **9**, 4115–4123 (2012).
35. Bottinga, Y. Calculated fractionation factors for carbon and hydrogen isotope exchange in the system calcite-carbon dioxide-graphite-methane-hydrogen-water vapor. *Geochim. Cosmochim. Acta* **33**, 49–64 (1969).
36. Rahn, T. et al. Extreme deuterium enrichment in stratospheric hydrogen and the global atmospheric budget of H_2. *Nature* **424**, 918–921 (2003).
37. Röckmann, T., Rhee, T. S. & Engel, A. Heavy hydrogen in the stratosphere. *Atmos. Chem. Phys.* **3**, 2015–2023 (2003).
38. Röckmann, T. et al. Isotopic composition of H_2 from wood burning: dependency on combustion efficiency, moisture content, and δD of local precipitation. *J. Geophys. Res. Atmos.* **115**, D17308 (2010).
39. Gerst, S. & Quay, P. Deuterium component of the global molecular hydrogen cycle. *J. Geophys. Res. Atmos.* **106**, 5021–5031 (2001).
40. Mußmann, M., Pjevac, P., Krüger, K. & Dyksma, S. Genomic repertoire of the Woeseiaceae/JTB255, cosmopolitan and abundant core members of microbial communities in marine sediments. *ISME J.* **11**, 1276–1281 (2017).
41. Greening, C. et al. Genomic and metagenomic surveys of hydrogenase distribution indicate H_2 is a widely utilised energy source for microbial growth and survival. *ISME J.* **10**, 761–777 (2016).
42. Søndergaard, D., Pedersen, C. N. S. & Greening, C. HydDB: a web tool for hydrogenase classification and analysis. *Sci. Rep.* **6**, 34212 (2016).
43. Berney, M., Greening, C., Conrad, R., Jacobs, W. R. & Cook, G. M. An obligately aerobic soil bacterium activates fermentative hydrogen production to survive reductive stress during hypoxia. *Proc. Natl Acad. Sci. USA* **111**, 11479–11484 (2014).
44. Greening, C. & Cook, G. M. Integration of hydrogenase expression and hydrogen sensing in bacterial cell physiology. *Curr. Opin. Microbiol.* **18**, 30–38 (2014).
45. Carere, C. R. et al. Mixotrophy drives niche expansion of verrucomicrobial methanotrophs. *ISME J.* **11**, 2599–2610 (2017).
46. Tengölics, R. et al. Connection between the membrane electron transport system and Hyn hydrogenase in the purple sulfur bacterium, *Thiocapsa roseopersicina* BBS. *BBA Bioenerg.* **1837**, 1691–1698 (2014).
47. Kreutzmann, A.-C. & Schulz-Vogt, H. N. Oxidation of molecular hydrogen by a chemolithoautotrophic *Beggiatoa* strain. *Appl. Environ. Microbiol.* **82**, 2527–2536 (2016).
48. Schwartz, E., Fritsch, J. & Friedrich, B. *H_2-Metabolizing Prokaryotes* (Springer, Berlin, 2013).
49. Peters, J. W. et al. [FeFe]- and [NiFe]-hydrogenase diversity, mechanism, and maturation. *BBA Mol. Cell Res.* **1853**, 1350–1369 (2015).
50. Banat, I. M., Lindström, E. B., Nedwell, D. B. & Balba, M. T. Evidence for coexistence of two distinct functional groups of sulfate-reducing bacteria in salt marsh sediment. *Appl. Environ. Microbiol.* **42**, 985–992 (1981).
51. Dong, X. et al. Fermentative Spirochaetes mediate necromass recycling in anoxic hydrocarbon-contaminated habitats. *ISME J.* **12**, 2039–2050 (2018).
52. Amin, S. A., Parker, M. S. & Armbrust, E. V. Interactions between diatoms and bacteria. *Microbiol. Mol. Biol. Rev.* **76**, 667–684 (2012).
53. Bullister, J. L., Guinasso, N. L. Jr & Schink, D. R. Dissolved hydrogen, carbon monoxide, and methane at the CEPEX site. *J. Geophys. Res. C* **87**, 2022–2034 (1982).
54. Lilley, M. D., Baross, J. A. & Gordon, L. I. Dissolved hydrogen and methane in Saanich Inlet, British Columbia. *Deep. Sea Res. A* **29**, 1471–1484 (1982).
55. Precht, E., Franke, U., Polerecky, L. & Huettel, M. Oxygen dynamics in permeable sediments with wave-driven pore water exchange. *Limnol. Oceanogr.* **49**, 693–705 (2004).
56. Kessler, A. J., Glud, R. N., Cardenas, M. B. & Cook, P. L. M. Transport zonation limits coupled nitrification–denitrification in permeable sediments. *Environ. Sci. Technol.* **47**, 13404–13411 (2013).
57. Arnosti, C., Ziervogel, K., Ocampo, L. & Ghobrial, S. Enzyme activities in the water column and in shallow permeable sediments from the northeastern Gulf of Mexico. *Estuar. Coast. Shelf Sci.* **84**, 202–208 (2009).
58. Grunwald, M. et al. Nutrient dynamics in a back barrier tidal basin of the Southern North Sea: Time-series, model simulations, and budget estimates. *J. Sea Res.* **64**, 199–212 (2010).
59. Kappelmann, L. et al. Polysaccharide utilization loci of North Sea Flavobacteriia as basis for using SusC/D-protein expression for predicting major phytoplankton glycans. *ISME J.* **13**, 76–91 (2019).
60. Du, Z.-J., Wang, Z.-J., Zhao, J.-X. & Chen, G.-J. *Woeseia oceani* gen. nov., sp. nov., a chemoheterotrophic member of the order Chromatiales, and proposal of Woeseiaceae fam. nov. *Int. J. Syst. Evol. Microbiol.* **66**, 107–112 (2016).
61. Constant, P., Chowdhury, S. P., Pratscher, J. & Conrad, R. Streptomycetes contributing to atmospheric molecular hydrogen soil uptake are widespread and encode a putative high-affinity [NiFe]-hydrogenase. *Environ. Microbiol.* **12**, 821–829 (2010).
62. Myers, M. R. & King, G. M. Isolation and characterization of *Acidobacterium ailaaui* sp. nov., a novel member of Acidobacteria subdivision 1, from a geothermally heated Hawaiian microbial mat. *Int. J. Syst. Evol. Microbiol.* **66**, 5328–5335 (2016).
63. Canfield, D. E. et al. A cryptic sulfur cycle in oxygen-minimum–zone waters off the Chilean coast. *Science* **330**, 1375–1378 (2010).
64. Novelli, P. C., Crotwell, A. M. & Hall, B. D. Application of gas chromatography with a pulsed discharge helium ionization detector for measurements of molecular hydrogen in the atmosphere. *Environ. Sci. Technol.* **43**, 2431–2436 (2009).
65. Rhee, T. S., Mak, J., Röckmann, T. & Brenninkmeijer, C. A. M. Continuous-flow isotope analysis of the deuterium/hydrogen ratio in atmospheric hydrogen. *Rapid Commun. Mass Spectrom.* **18**, 299–306 (2004).
66. Chen, Q., Popa, M. E., Batenburg, A. M. & Röckmann, T. Isotopic signatures of production and uptake of H_2 by soil. *Atmos. Chem. Phys.* **15**, 13003–13021 (2015).
67. Bankevich, A. et al. SPAdes: a new genome assembly algorithm and its applications to single-cell sequencing. *J. Comput. Biol.* **19**, 455–477 (2012).
68. Kang, D. D., Froula, J., Egan, R. & Wang, Z. MetaBAT, an efficient tool for accurately reconstructing single genomes from complex microbial communities. *PeerJ* **3**, e1165 (2015).
69. Wu, Y.-W., Tang, Y.-H., Tringe, S. G., Simmons, B. A. & Singer, S. W. MaxBin: an automated binning method to recover individual genomes from metagenomes using an expectation-maximization algorithm. *Microbiome* **2**, 26 (2014).
70. Imelfort, M. et al. GroopM: an automated tool for the recovery of population genomes from related metagenomes. *PeerJ* **2**, e603 (2014).
71. Sieber, C. M. K. et al. Recovery of genomes from metagenomes via a dereplication, aggregation and scoring strategy. *Nat. Microbiol.* **3**, 836–843 (2018).
72. Olm, M. R., Brown, C. T., Brooks, B. & Banfield, J. F. dRep: a tool for fast and accurate genomic comparisons that enables improved genome recovery from metagenomes through de-replication. *ISME J.* **11**, 2864 (2017).
73. Parks, D. H., Imelfort, M., Skennerton, C. T., Hugenholtz, P. & Tyson, G. W. CheckM: assessing the quality of microbial genomes recovered from isolates, single cells, and metagenomes. *Genome Res.* **25**, 1043–1055 (2015).
74. Bowers, R. M. et al. Minimum information about a single amplified genome (MISAG) and a metagenome-assembled genome (MIMAG) of bacteria and archaea. *Nat. Biotechnol.* **35**, 725–731 (2017).
75. Lagesen, K. et al. RNAmmer: consistent and rapid annotation of ribosomal RNA genes. *Nucleic Acids Res.* **35**, 3100–3108 (2007).
76. Pruesse, E., Peplies, J. & Glöckner, F. O. SINA: accurate high-throughput multiple sequence alignment of ribosomal RNA genes. *Bioinformatics* **28**, 1823–1829 (2012).
77. Quast, C. et al. The SILVA ribosomal RNA gene database project: improved data processing and web-based tools. *Nucleic Acids Res.* **41**, D590–D596 (2012).

78. Parks, D. H. et al. A standardized bacterial taxonomy based on genome phylogeny substantially revises the tree of life. *Nat. Biotechnol.* **36**, 996–1004 (2018).
79. Nguyen, L.-T., Schmidt, H. A., von Haeseler, A. & Minh, B. Q. IQ-TREE: a fast and effective stochastic algorithm for estimating maximum-likelihood phylogenies. *Mol. Biol. Evol.* **32**, 268–274 (2014).
80. Hyatt, D. et al. Prodigal: prokaryotic gene recognition and translation initiation site identification. *BMC Bioinformatics* **11**, 119 (2010).
81. Eddy, S. R. Accelerated profile HMM searches. *PLoS Comput. Biol.* **7**, e1002195 (2011).
82. Boyd, J. A., Woodcroft, B. J. & Tyson, G. W. GraftM: a tool for scalable, phylogenetically informed classification of genes within metagenomes. *Nucleic Acids Res.* **46**, e59–e59 (2018).
83. Schloss, P. D. et al. Introducing mothur: open-source, platform-independent, community-supported software for describing and comparing microbial communities. *Appl. Environ. Microbiol.* **75**, 7537–7541 (2009).
84. Caporaso, J. G. et al. Global patterns of 16S rRNA diversity at a depth of millions of sequences per sample. *Proc. Natl Acad. Sci. USA* **108**, 4516–4522 (2011).
85. Amir, A. et al. Deblur rapidly resolves single-nucleotide community sequence patterns. *mSystems* **2**, e00191–16 (2017).
86. Callahan, B. J., McMurdie, P. J. & Holmes, S. P. Exact sequence variants should replace operational taxonomic units in marker-gene data analysis. *ISME J.* **11**, 2639 (2017).
87. Anantharaman, K. et al. Thousands of microbial genomes shed light on interconnected biogeochemical processes in an aquifer system. *Nat. Commun.* **7**, 13219 (2016).
88. Anantharaman, K. et al. Expanded diversity of microbial groups that shape the dissimilatory sulfur cycle. *ISME J.* **12**, 1715–1728 (2018).
89. Larkin, M. A. et al. Clustal W and Clustal X version 2.0. *Bioinformatics* **23**, 2947–2948 (2007).
90. Kumar, S., Stecher, G. & Tamura, K. MEGA7: Molecular Evolutionary Genetics Analysis version 7.0 for bigger datasets. *Mol. Biol. Evol.* **33**, 1870–1874 (2016).
91. Fonselius, S., Dyrssen, D. & Yhlen, B. in *Methods of Seawater Analysis* 3rd edn (eds Grasshoff, K., Kremling, K. & Ehrhardt, M.), 91–100 (Wiley, 2007).
92. Guillard, R. R. L. & Ryther, J. H. Studies of marine planktonic diatoms: I. *Cyclotella nana* Hustedt, and *Detonula confervacea* (Cleve) Gran. *Can. J. Microbiol.* **8**, 229–239 (1962).
93. Paulin, M. M. et al. Improving Griffith's protocol for co-extraction of microbial DNA and RNA in adsorptive soils. *Soil Biol. Biochem.* **63**, 37–49 (2013).

Acknowledgements

This study was funded by an ARC Discovery Project (DP180101762; awarded to P.L.M.C. and C.G.), an ARC DECRA Fellowship (DE170100310; awarded to C.G.) and an ARC Laureate Fellowship (FL150100038; awarded to P.H.). Y.-J.C. was supported by PhD scholarships from Monash University and the Taiwan Ministry of Education. We thank T. Röckmann for supporting the isotope fractionation work, R. Glud for helpful discussions that led to the conception of this project, and K. Handley and M. Mußmann for their helpful insights. We also acknowledge V. Eate, D. Brehm, L. Stoop, T. Jirapanjawat, S. Davy-Prefumo, S. Bay, R. Pierson and M. Raveggi for providing field and technical support.

Author contributions

P.L.M.C., C.G. and A.J.K. conceived, designed and supervised this study. Different authors were responsible for in situ measurements (Y.-J.C., A.J.K., S.K., P.L.M.C., T.H. and C.G.), isotope mass spectrometry analysis (M.E.P., A.J.K. and P.L.M.C.), diatom experiments (Y.-J.C., J.B., C.G. and P.L.M.C.), FTR experiments (A.J.K., S.K. and P.L.M.C.), slurry experiments (T.H., Y.-J.C., A.J.K., P.L.M.C. and C.G.), community analysis (Y.-J.C., D.W.W., C.G. and P.H.) and functional gene analysis (D.W.W., C.G., P.H. and Y.-J.C.). C.G., A.J.K., Y.-J.C., P.L.M.C. and D.W.W. analysed the data and wrote the paper with input from all authors.

Competing interests

The authors declare no competing interests.

Additional information

Supplementary information is available for this paper at https://doi.org/10.1038/s41564-019-0391-z.

Reprints and permissions information is available at www.nature.com/reprints.

Correspondence and requests for materials should be addressed to P.L.M.C. or C.G.

Publisher's note: Springer Nature remains neutral with regard to jurisdictional claims in published maps and institutional affiliations.

nature research

Corresponding author(s): Chris Greening & Perran Cook

Reporting Summary

Nature Research wishes to improve the reproducibility of the work that we publish. This form provides structure for consistency and transparency in reporting. For further information on Nature Research policies, see Authors & Referees and the Editorial Policy Checklist.

Statistical parameters

When statistical analyses are reported, confirm that the following items are present in the relevant location (e.g. figure legend, table legend, main text, or Methods section).

n/a	Confirmed	
☐	☒	The exact sample size (*n*) for each experimental group/condition, given as a discrete number and unit of measurement
☐	☒	An indication of whether measurements were taken from distinct samples or whether the same sample was measured repeatedly
☒	☐	The statistical test(s) used AND whether they are one- or two-sided *Only common tests should be described solely by name; describe more complex techniques in the Methods section.*
☒	☐	A description of all covariates tested
☒	☐	A description of any assumptions or corrections, such as tests of normality and adjustment for multiple comparisons
☐	☒	A full description of the statistics including central tendency (e.g. means) or other basic estimates (e.g. regression coefficient) AND variation (e.g. standard deviation) or associated estimates of uncertainty (e.g. confidence intervals)
☒	☐	For null hypothesis testing, the test statistic (e.g. *F*, *t*, *r*) with confidence intervals, effect sizes, degrees of freedom and *P* value noted *Give P values as exact values whenever suitable.*
☒	☐	For Bayesian analysis, information on the choice of priors and Markov chain Monte Carlo settings
☒	☐	For hierarchical and complex designs, identification of the appropriate level for tests and full reporting of outcomes
☐	☒	Estimates of effect sizes (e.g. Cohen's *d*, Pearson's *r*), indicating how they were calculated
☐	☒	Clearly defined error bars *State explicitly what error bars represent (e.g. SD, SE, CI)*

Our web collection on statistics for biologists may be useful.

Software and code

Policy information about availability of computer code

Data collection	PeakSimple 2000 chromatography integration software (SRI instrument, CA, USA) Isodat^TM 2 (Thermo Fisher Scientific, USA) Pyro Oxygen Logger (PyroScience, Germany)
Data analysis	BamM v1.7.3 BBTools v36.92 (https://sourceforge.net/projects/bbmap/) CheckM v1.0.11 ClustalX DAS_Tool v1.1.1 deblur Diamond dRep v2.0.5 GraftM GroopM v0.3.0 GTDB-TK pipeline hmmer v3.1b2 IQ-Tree LSU v132 database MaxBin v.2.2.4

MEGA7
MetaBat v2.12.1
mother v.132 database
Panther database
PeakSimple 2000
Pfam v31.0 database
Prodigal v2.6.3
QIIME 2 platform version 2018.4 (https://qiime2.org/)
RefineM
RNAmmer v1.2
SILVA SSU database
SINA web aligner
SPAdes v.3.11.1
TIGRfam v15.0 database
v132 database

For manuscripts utilizing custom algorithms or software that are central to the research but not yet described in published literature, software must be made available to editors/reviewers upon request. We strongly encourage code deposition in a community repository (e.g. GitHub). See the Nature Research guidelines for submitting code & software for further information.

Data

Policy information about availability of data

All manuscripts must include a data availability statement. This statement should provide the following information, where applicable:

- Accession codes, unique identifiers, or web links for publicly available datasets
- A list of figures that have associated raw data
- A description of any restrictions on data availability

Community data based on shotgun metagenome sequencing and amplicon sequencing are provided as supporting information (Table S1 & S2). In addition, the metagenomes and metagenome-assembled genomes have been deposited on to public servers and accession codes provided. All other data that support the findings of this study are available from the corresponding author upon reasonable request.

Field-specific reporting

Please select the best fit for your research. If you are not sure, read the appropriate sections before making your selection.

☐ Life sciences ☐ Behavioural & social sciences ☒ Ecological, evolutionary & environmental sciences

For a reference copy of the document with all sections, see nature.com/authors/policies/ReportingSummary-flat.pdf

Ecological, evolutionary & environmental sciences study design

All studies must disclose on these points even when the disclosure is negative.

Study description

This study describes the metabolic cycling of H2 in permeable sediments. In particular, we show through a combination of in-situ measurements and flow-through reactor and slurry experiments that H2 accumulates in sandy sediments due to decoupling of production by fermentative bacteria at the onset of anoxia and aerobic respiratory H2 consumption. Community and metagenomic profiling of the sediments reveal that abundant [NiFe]-hydrogenases among facultatively fermentative bacteria facilitate this H2 cycling in an environment with varying oxygen availability.

δ2H-H2 of seawater was determined with 10 single measurements (n=1) during one day. Pore water H2 concentrations were determined from the average of three separate sediment cores (n=3). Flow-through reactor (n=3) and slurry (n=3-6) experiments were prepared using subsamples of homogenised surface sediment collected on the corresponding sampling days. Metagenomes (n=5) were prepared using samples collected from intertidal samples (2-5 cm, 15-18 cm), subtidal samples (2-5 cm, 15-18 cm) flow-through reactor samples.

Research sample

Seawater and sediment samples collected from Port Phillip Bay, Melbourne, Australia were used in this study. All microbial and biogeochemical work was performed on these samples. This site is chosen because it has previously been shown that the sediments from here produce large amounts of H2 gas (Bourke et al., Nat. Geo., 2017). We do not propose that this site is representative of any larger system, and use this site as a model to showcase this novel metabolism.

Sampling strategy

For seawater samples, 500 mL water samples were drawn up from approximately 50 cm below the surface using a 1.6 L polycarbonate syringe. The remainder of the syringe was filled with ambient air. The syringe was then sealed and shaken vigorously for 2 minutes to transfer the H2 to the gas phase. The headspace was transferred to an evacuated 1 L glass flask for later analysis.

Due to the expensive and time-consuming nature of δ2H-H2 analysis, no replicates were performed for this work (i.e. n=1).
For sediment collection, samples were collected from well-mixed silicate sands from both the subtidal zone (~ 1 m deep at low tide) and intertidal zone (~ 1 m deep at high tide) using polyacrylamide cores (20 cm depth, 6.7 cm ID). These samples were then transferred to flow-through reactors (n = 3) and/or slurry reactors (n = 3-6, see Materials and Methods), or preserved for microbial analysis.

For sediment depth profiles, three sediment cores of 20 cm depth were collected from subtidal sands. Cores were carefully extruded and segmented into 2 cm slices. They were immediately transferred to beakers containing 30 mL Ar-purged carbonate-free artificial seawater supplemented with 2 % ZnCl2. The slices were gently stirred to homogenize the porewater with the artificial seawater. 3 mL of the solution was transferred to a gas tight vial and 1.5 mL of the liquid was replaced with a He headspace.

For flow-through reactor, slurry and sediment depth profile experiments, at least three replicates were performed so that the uncertainty in our measurements could be determined. This is the standard sample size for geomicrobiological studies, and the results show that the treatments vary to such an extent that this replication is sufficient. No statistical methods were used to pre-determine sample size.

Data collection

Samples were collected by the authors as described above, and all data were recorded digitally or analysed computationally as follows.

- H2 was measured by an SRI Model 8610 Gas Chromatograph or a Valco TGA-6791-W-4U-2 Trace Gas Analyzer.
- δ2H-H2 was measured using a ThermoFinnigan Delta Plus XL.
- δ2H-H2O was measured using a Thermo Finnigan H-Device coupled to a Thermo Finnigan Delta Plus Advantage gas source mass spectrometer.
- Shotgun metagenomic sequencing was performed on an Illumina NextSeq500 platform and analysed using BBDuk, GratM, mothur, hmmer, DIAMOND, and MEGA7.
- Metagenome-assembled genomes were assembled and analyzed using SPAdes, BamM, MetaBAT, MaxBin, GroopM, DAS_Tool, dRep, CheckM, RefineM, RNAmmer, GTDB-TK, and Prodigal.
- 16 rRNA gene amplicons were sequenced using an Illumina MiSeq and analysed using the deblur pipeline on the QIIME 2 platform.
- O2 was measured using a Pyroscience Firesting optical probe.
- H2S was measured using a GBC UV/Visible Spectrophotometer using the methylene blue method.
- 15N2 production was analyzed using a Sercon isotope ratio mass spectrometer coupled to a gas chromatograph.

Different authors were responsible for in situ measurements (Y.J.C., A.J.K., S.K., P.L.M.C., T.H., C.G.), isotope mass spectrometry analysis (M.E.P., A.J.K., P.L.M.C.), diatom experiments (Y.J.C., J.B., C.G., P.L.M.C.), flow-through reactor experiments (A.J.K., S.K., P.L.M.C.), slurry experiments (T.H., Y.J.C., A.J.K., P.L.M.C., C.G.), community analysis (Y.J.C., D.W., C.G., P.H.), and functional gene analysis (D.W., C.G., P.H., Y.J.C.). C.G., A.J.K., Y.-J.C., P.L.M.C., and D.W. analyzed the data.

Timing and spatial scale

All sample collections were conducted at Middle Park Beach, Melbourne, Australia (37.852425 S, 144.957519 E).

Seawater samples were collected from beyond the wash zone (~1 m deep) on October 28, 2016. Samples were collected every hour over an 11-hour period that encompassed low tide and high tide. This timing was chosen in order to observe any changes with tide.

Sediment samples for metagenome sequencing, and flow-through reactor experiments were collected on October 28, 2016. Samples for successive slurry experiments were collected on April 10, 2018 (experiment 1), April 30, 2018 (experiment 2), June 20, 2018 (experiment 3), or October 22, 2018 (experiment 4). Sediment samples for depth profiles were collected on February 28, 2018.

Flow-through reactor experiments were performed until H2 was no longer observed and H2S production dominated. Slurry experiments were performed until H2 concentrations were stable at equilibrium concentration.

Data exclusions

No data were excluded from the manuscript. For the Keeling plot on Figure 1c, an outlying value (9 am) time point was excluded that is shown in Figure 1b.

Reproducibility

Experiments were performed periodically from October 2016 to October 2018, and similar results are obtained throughout this period. All attempts to repeat aspects of experiments were successful, and are included herein.

Randomization

Where samples were collected on site, we returned to the same site throughout the period described. Where samples were returned to the laboratory for flow-through reactor or slurry experiments, samples were homogenized and sub-sampled for the various treatments.

Blinding

As our study describes microbial processes and all data were collected using automated, digital instruments, blinding was not necessary in our experimental design.

Did the study involve field work? ☒ Yes ☐ No

Field work, collection and transport

Field conditions

Middle Park Beach is situated in Port Phillip Bay, ~ 5 km from the central business district of Melbourne, Australia. The site is accessible to general public. Port Phillip Bay is a relatively large, shallow embayment (1930km2, mostly < 8 m deep, max depth 24 m) which provides protection to its beaches from severe weather. Seawater temperature ranged from 13.6 to 20.3°C based on historical record (https://www.seatemperature.org/australia-pacific/australia/port-phillip.htm).

Location

All sample collections were conducted at Middle Park Beach, Melbourne, Australia (37.852425 S, 144.957519 E). All samples were collected manually in fine weather from shallow (~ 1m deep) water less than 30 m from shore.

Access and import/export

Suitable footwear, gloves and equipments were used during the sampling process to minimize anthropogenic effects.

Disturbance

In total, <10 L of porewater and <10 kg of sediment samples were collected for this from the nearshore samplng. Disturbance was negligible as small volumes of samples were collected from a large beach in an urbanised area and any sediment taken will be replaced during tidal flows. In addition, appropriate cores and syringes were used.

Reporting for specific materials, systems and methods

Materials & experimental systems

n/a	Involved in the study
☒	☐ Unique biological materials
☒	☐ Antibodies
☒	☐ Eukaryotic cell lines
☒	☐ Palaeontology
☒	☐ Animals and other organisms
☒	☐ Human research participants

Methods

n/a	Involved in the study
☒	☐ ChIP-seq
☒	☐ Flow cytometry
☒	☐ MRI-based neuroimaging